ELSEVIER

Temperature distribution measurement on microfabricated thermodevice for single biomolecular observation using fluorescent dye

Hideyuki F. Arata [a,*], Peter Löw [b,c], Koji Ishizuka [d], Christian Bergaud [b],
Beomjoon Kim [a], Hiroyuki Noji [e], Hiroyuki Fujita [a]

[a] *Institute of Industrial Science (IIS), The University of Tokyo, 4-6-1 Komaba, Meguro-ku, Tokyo 153-8505, Japan*
[b] *LIMMS-CNRS/IIS, Institute of Industrial Science (IIS), The University of Tokyo, 4-6-1 Komaba, Meguro-ku, Tokyo 153-8505, Japan*
[c] *LAAS-CNRS, 7 Avenue du Colonel Roche, 31077 Toulouse Cedex 4, France*
[d] *Department of Electronic Chemistry, Tokyo Institute of Technology, 4259 Nagatsuta-cho, Midori-ku, Yokohama 226-8502, Japan*
[e] *Institute of Scientific and Industrial Research (ISIR), The Osaka University, Mihogaoka 8-1, Ibaraki, Osaka 567-0047, Japan*

Abstract

Precise temperature distribution measurements with high spatial resolution are of great importance in bioassay which uses microfabricated thermodevice, such as single biomolecular observation. We propose a new method to measure the temperature distribution in water with high spatial resolution using the fluorescent dye, Rhodamine B. Since Rhodamine B solution exhibits a strong and reversible temperature-dependent variation in its fluorescent intensity, it is useful as a temperature detector. The temperature distribution on a microfabricated thermodevice was successfully calculated from the fluorescent intensity distribution of a Rhodamine B solution. Finite element method modeling was carried out to demonstrate the reliability of the proposed method. A comparison between the measured and simulated temperature distributions revealed an excellent agreement. The method allows for direct measurement of the local temperature on our microfabricated thermodevice, where the molecule of interest stands, with an accuracy of 3 °C and a spatial resolution of 5.3 μm. Precise temperature detection along with optical measurement was possible due to our new method to detect temperature distribution. This is a promising method to reveal the temperature dependent characteristics of F_1-ATPase in future study. Applying this method to other single molecular observations might also realize reliable temperature measurement and may achieve substantial results.
© 2005 Elsevier B.V. Open access under CC BY-NC-ND license.

Keywords: Rhodamine B; Temperature distribution; Fluorescent dye; Single molecular observation; Microheater

1. Introduction

The measurement of protein molecules has commonly been performed as an average over a large number of molecules in biochemistry. Recently, the direct observation of an individual molecule has enabled the interpretation of its individual behavior and characteristics [1]. This is a cutting-edge technique in molecular biology. The development of tools suitable for single molecule handling and its characterization is one of the key issues for further progress. The size of a protein is of the order of nanometers. Minute structured tools are required to work with these proteins. Micro- and nanotechnologies of today offer an opportunity to develop such tools, making it possible to perform quantiative novel experiments, and to produce results and knowledge that would not otherwise be accessible.

In earlier research of ours, the temperature-dependent activity of a single biomolecule was studied using a MEMS-based microfabricated thermodevice [2,3]. In such kinds of works, temperature accuracy of 5 °C as well as spatial resolution of a few micrometers is required. Fig. 1 shows our system for single biomolecular observation, a rotary assay of F_1-ATPase. The device consists of microfabricated heater and thermodevice which are integrated in the flow chamber which they use for the conventional bioassay. The absolute accuracy of the thermosensor itself is 1 °C. Thus far, however, we could not measure the temperature in high spatial resolution due to the difficulty in measuring the temperature distribution in water. An infrared camera can be used to measure the temperature distri-

* Corresponding author.
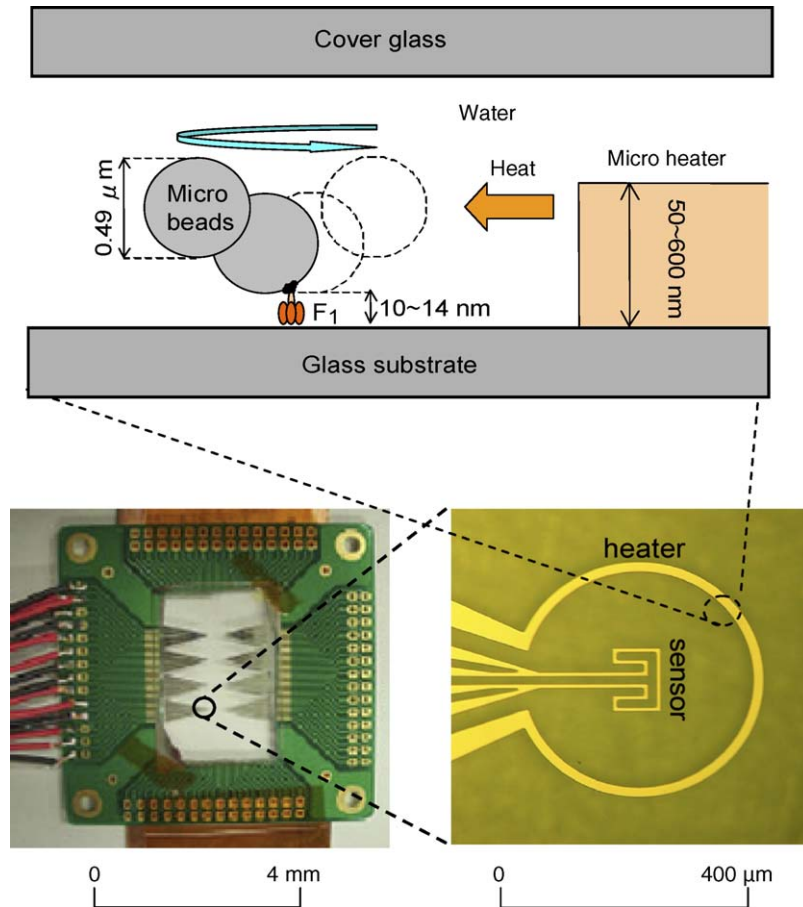 *E-mail address:* arata@iis.u-tokyo.ac.jp (H.F. Arata).

Fig. 1. Single biomolecular observation, a rotation assay of a F_1-ATPase, carried out on the microfabricated thermodevice (top). A MEMS-based microfabricated thermodevice which allows rapid temperature control under the microscope for single molecular observation (bottom). The integrated microfabricated thermosensor can detect the average temperature at the center of the circular microheater, whose diameter is 400 μm. However, the spatial resolution is poor since it cannot measure the temperature distribution.

bution with a spatial resolution of a few micrometers; however, it cannot be used for measurements on wet materials because water absorbs infrared light. A thermometer integrated in a microscale can measure the temperature in water but with poor spatial resolution. In this report, we propose a new method to measure the temperature distribution in water with high spatial resolution using a fluorescent dye. This enables us to measure the temperature distribution proceeding to the biomolecular assay.

2. Materials

Fluorescent materials such as Rhodamine B, Fluorescein, thermochromic liquid crystals (TLC) [4,5] and Quantum dots (Qdots) [6] exhibit temperature-dependent light intensities. Thanks to this, they can be used as probes to measure the temperature by calibrating the relationship between their light intensity and the temperature. However, the relation between fluorescent intensity and temperature of the plastic beads that contain the fluorescent dye on its surface is not reversible over 60 °C (Fig. 2) because the temperature stability of the plastic beads is lower than 60 °C. The measurable temperature for the TLC is limited in the range of 55–75 °C [4,5].

In the case of Qdots, the intensity is highly linear with temperature. However, the earlier study reports that the maximum temperature of Qdots is 60 °C, above which they lose their reversibility [6]. We carried out the experiment to confirm the temperature stability of Qdots using the microsystems which we used in our previous studies; microchamber and microheater [7] together with microneedle [8,9]. Qdot (#1002-1J, Quantum Dot
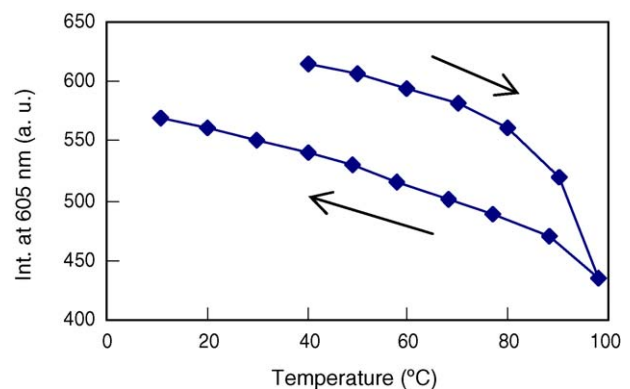

Fig. 2. Fluorescent intensity vs. temperature for fluorescent dye contained in plastic beads. The fluorescent intensity is not reversible since the plastic beads lose their physical property permanently at temperature higher than 60 °C.
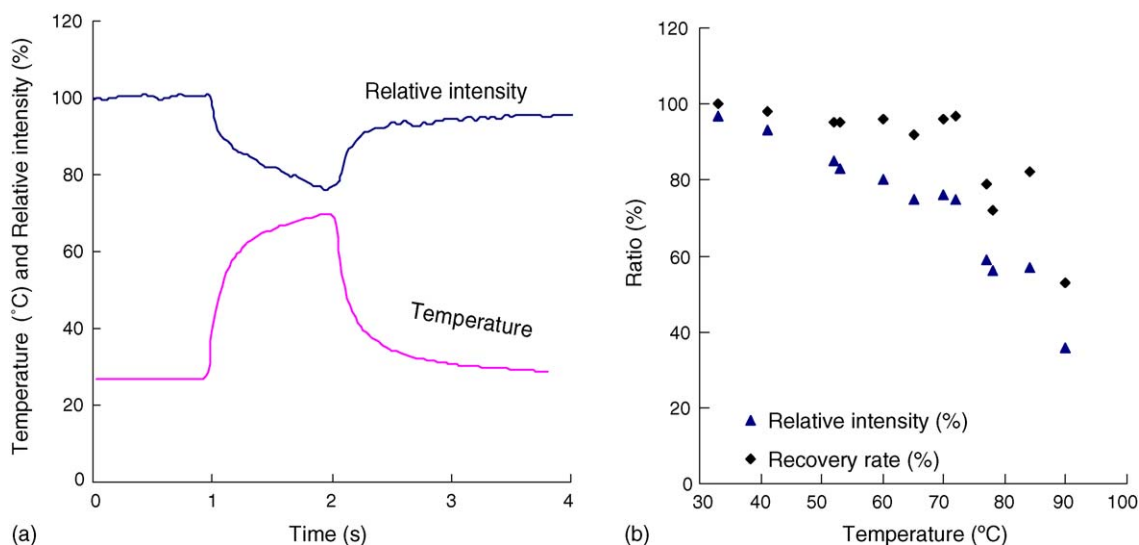
Fig. 3. (a) Time course of fluorescent intensity of Qdots during temperature alternation. (b) Relative intensity compared with the intensity at room temperature (triangle) and recovery rate after inducing heat pulses at each temperature (diamond).

Corporation) was diluted in the 50 mM MOPS-KOH buffer (pH 7.0, with 5% Tween20 to avoid absorption to the wall of the PDMS chambers) and poured 5 μL in a flow cell on a microheater. A flow cell was constructed with glued parafilm sandwiched by microfabricated PDMS sheet and glass plate. The size of a chamber is cylinder shape with 6 μm in diameter and 1.5 μm in height. Qdots were confined in the microchamber by pushing the PDMS sheet with the needle (40 μm in diameter) as we confined enzymes in our previous works [8,9]. Filters (BP330–385 and BA580IF: Olympus) were used to observe fluorescent intensity of Qdots under the microscope (IX71: Olympus). The CCD camera (CCD-300RCX) detects the image via image intensifier (C8600–05: Hamamatsu). Average fluorescent intensity in one microchamber was analyzed by the software (CREST Image). The heat pulses were induced by the microheater. The fluorescent intensity of Qdots decreases when the temperature is raised (Fig. 3a). The recovery rates after inducing a heat pulse are shown in Fig. 3b. The recovery rates keeps near 100% under

70 °C but reduces drastically over 70 °C. This results shows that, in our condition, 70 °C is the maximum temperature which we can use Qdots as a temperature detector.

On the other hand, the fluorescent intensity of Rhodamine B and Fluorescein in water solution is highly reversible in relation to the temperature (Fig. 4) [10,11]. Hence, we selected Rhodamine B solution as the temperature detector since it is cost less than Fluorescein.

3. Experimental

The device and schematic are shown in Fig. 1. The micro heater raises the temperature of the water in a local area through Joule heating. The microfabricated thermosensor measures the temperature based on its temperature-dependent resistance. A calibration curve of the integrated thermosensor was obtained by immersing it into a water bath. The accuracy of the thermosensor calibrated by this method was 1 °C. In order to calculate the temperature from the fluorescent intensity of a Rhodamine B solution, we determine the calibration curve between the temperature and the fluorescent intensity beforehand. This calibration was carried out under the microscope. A fluorescent intensity of the peripheral area of the integrated thermosensor was measured which corresponds to the temperature detected by the thermosensor. The reversibility of the calibration curve depends on the evaporation of the water solvent as the concentration of Rhodamine B increases when the water evaporates. The accuracy of this calibration curve was better than 0.3 °C during 15-min measurements, and this accuracy is acceptable in our experiments.

We filled the flow chamber, in which microheaters and microsensors are integrated, with Rhodamine B solution (Wako; 183-00122, 100 μM). The microheater locally warms the surface of the glass plate, and the diffusion of heat produces the steady-state temperature distribution. The Rhodamine B solution was excited by a mercury lamp through a band pass filter (WIG, BP
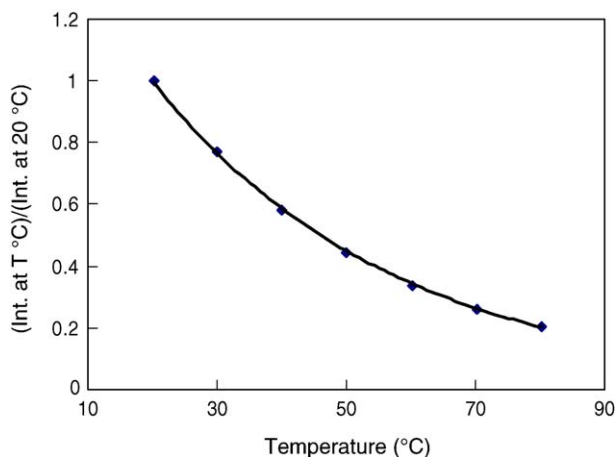

Fig. 4. The fluorescent intensity of Rhodamine B solution depends on the temperature. Its characteristic is highly reversible and is useful as a temperature detector.

520–550: Olympus) and an ND filter (ND12) which reduces the intensity of excitation light. The duration of each exposure to the excitation light was 1/8 s. The reason to use pulsed exposure was to minimize the fluorescent quenching effect. With this technique, the intensity at steady temperature was found to drift by 0.5% after 10 exposures. A fluorescent image was captured with a CCD camera (HAMAMATSU: IR-CCD) and recorded on a digital video cassette (SONY: MiniDV). The intensity was analyzed using a free software (ScionImage). The fluorescent intensity distribution was converted to determine the temperature distribution using the calibration curve.

4. Results and discussion

The temperature distribution around the microheater was successfully calculated from the intensity distribution of the rhodamine B solution. Fig. 5 shows a microscopic view when the thermosensor indicates 68 °C (a), 51 °C (b), 37 °C (c) and 27 °C (d). Fig. 4(e) shows the 3D image of the temperature distribution calculated from the distribution of the fluorescent intensity when the integrated thermosensor indicates 68 °C. The cross-sectional temperature distribution along the line A–B in Fig. 5(e) is shown in Fig. 5(f).

The reproducibility of this temperature distribution detection method is 2 °C, it was measured from the reproducibility of the fluorescent intensity under identical temperature conditions. The spatial resolution is equal to the width of a pixel of the measured value; in this experiment, it was 5.3 µm. When the temperature at the center of the circular heater was approximately 70 °C, the temperature variation inside the circular heater was measured to be smaller than 2 °C. The temperature variation was found to decrease with the temperature at the center of the circular heater. From this result, it can be concluded that the temperature of an observed target within the circular heater differs with less than 2 °C from that of the integrated thermosensor.

5. FEM modeling of the microheater

Since the proposed microheater is very simple in design, involving few materials and a simple geometry, it is straightforward to develop a finite element method (FEM) model in order to investigate its heating characteristics. A three-dimensional
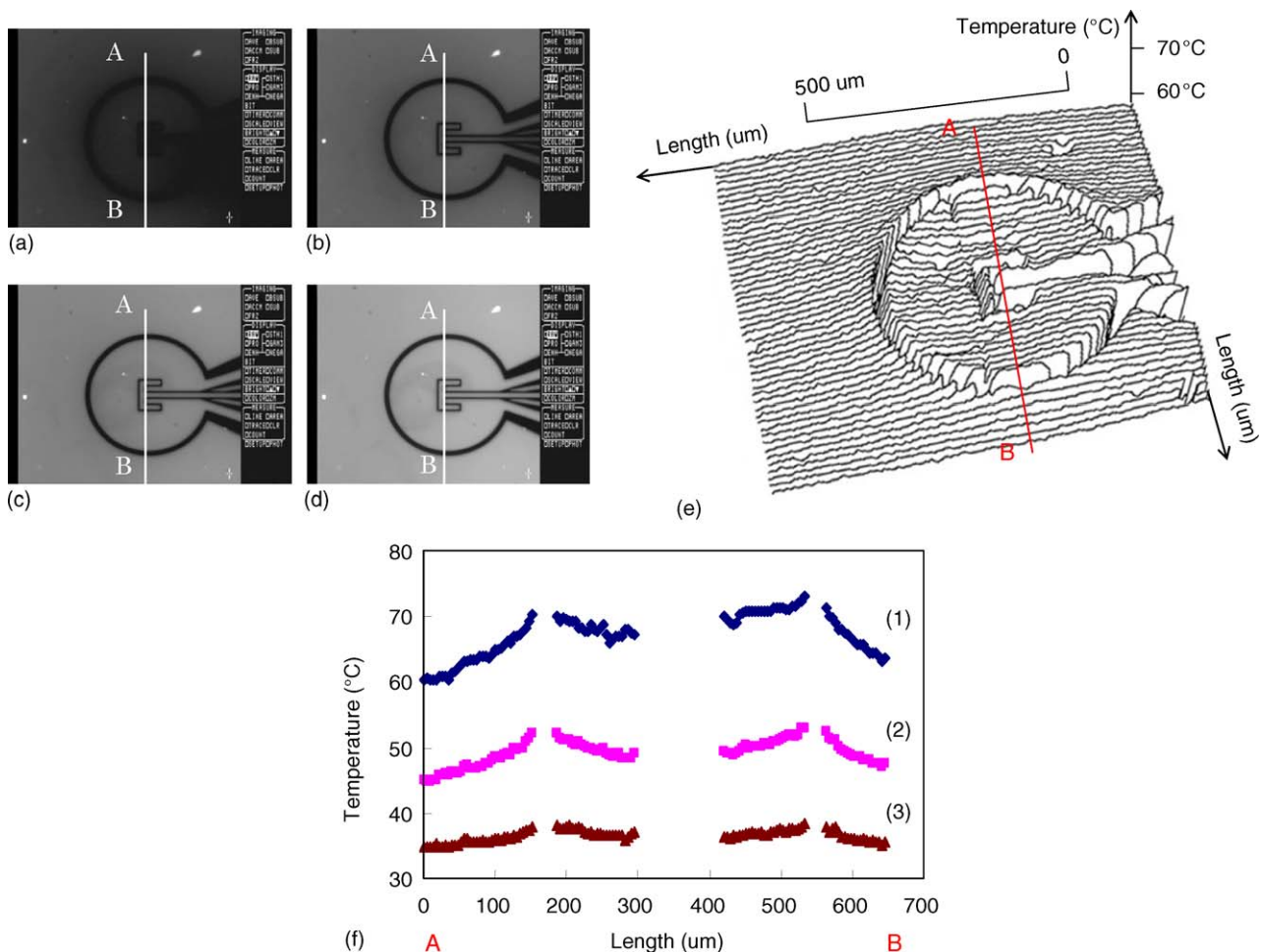

Fig. 5. Microscopic view when the thermosensor shows 68 °C (a), 51 °C (b), 37 °C (c) and 27 °C (d). (e) 3D image of the temperature distribution calculated from the distribution of the fluorescent intensity when the integrated thermosensor indicates 68 °C. (f) Cross-sectional temperature gradients. The X-axis represents the distance from point A shown in (a)–(e). The areas around 180 µm, from 300 to 400 µm and around 550 µm were subtracted since the micropatterned heater and sensor do not transmit fluorescent light. The data shows the gradient when the thermosensor indicates 68 °C (1), 51 °C (2) and 37 °C (3), respectively.

steady-state model of this type was implemented using the commercial software FEMLAB® (COMSOL, version 3.1). Assumptions made for the model and the simulation results will be presented in the following paragraphs.

When a voltage is applied to the microheater, Joule heating occurs throughout the nickel circuit. The subsequent heat transfer through the device can be expressed mathematically by the following formula:

$$Q = P_{\text{conduction}} + P_{\text{convection}} + P_{\text{radiation}}$$

where Q represents the produced heat per unit volume and $P_{\text{conduction}}$, $P_{\text{convection}}$ and $P_{\text{radiation}}$ represent the power losses per unit volume due to conduction, convection and radiation, respectively. Because of the low temperature range used for the heater ($<75\,^{\circ}$C), the radiation losses can be considered negligible [12–14]. Moreover, considering the small fluid volume surrounding the heater and the absence of an externally imposed flux, the convection losses can also be assumed to be negligible. Thus, these assumptions yield:

$$Q = P_{\text{conduction}}$$

The conduction losses in a steady state model are given by:

$$P_{\text{conduction}} = \nabla(-\kappa\nabla T)$$

where κ represents the thermal conductivity of the respective materials. In this study, we used $\kappa_{\text{Ni}} = 90.7\,\text{Wm}^{-1}\,^{\circ}\text{C}^{-1}$ for nickel and $\kappa_{\text{glass}} = 1.38\,\text{Wm}^{-1}\,^{\circ}\text{C}^{-1}$ for the glass substrate.

In order to simplify the model, the nickel track for heating was implemented using the built-in thin conductive layer mode in FEMLAB. By using this mode, the potential gradient along the vertical direction of the nickel layer can be assumed to be zero. This is a valid approximation in this study, since the thickness of the nickel layer is several magnitudes smaller than its width and length. Using this approximation, the total produced heat in the nickel layer is given by the following formula, where the index k represents the individual elements of the model:

$$Q = \sum_{k} d\sigma_k(T_k)(\nabla_t V)_k^2 S_k = d\sum_{k}\sigma(T_k)(\nabla_t V)_k^2 S_k$$

$$\sigma(T_k) = \frac{\sigma_0}{1 + \alpha(T_k - T_0)}$$

where d represents the thickness of the nickel layer, S_k represents the area of element, T_k represents the temperature in element k, $\sigma(T_k)$ represents the temperature-dependent electrical conductivity of nickel and $(V_t V)_k$ represents the horizontal electric potential drop in element k. In the formula for the electrical conductivity, σ_0 is the conductivity at $T_0 = 20\,^{\circ}$C and α is the temperature coefficient of the electrical resistivity. For nickel, the values of the conductivity and the temperature coefficient are $\sigma_0 = 1.45$ S/m and $\alpha = 0.0068\,^{\circ}\text{C}^{-1}$, respectively. As for the boundary conditions of the model, we assumed ambient temperature ($20\,^{\circ}$C) at the interface between the glass substrate and the surroundings (Dirichlet type conditions). On the top and bottom boundaries, we assumed an outward heat flux (Neumann type conditions). The heat flux was modeled using a heat transfer coefficient, h, giving the heat flux as power loss

per area unit and $^{\circ}$C of temperature difference between the inside and the outside of the boundary ($\text{W m}^{-2}\,^{\circ}\text{C}^{-1}$). For the upper boundary, at the water interface, a heat transfer coefficient $h_{\text{water}} = 20\,\text{W m}^{-2}\,^{\circ}\text{C}^{-1}$ was used representing heat losses to the water through conduction and diffusive convection. At the lower boundary, representing natural convection of air, $h_{\text{air}} = 5\,\text{W m}^{-2}\,^{\circ}\text{C}^{-1}$ was used. In order to create a mesh for the FEM analysis, a two-dimensional geometry was initially drawn. A triangular mesh was automatically generated by FEMLAB. Manual extrusion of the two-dimensional mesh rendered the final three-dimensional mesh geometry on which FEM analysis could be performed.

The result of the implemented model is shown in Fig. 6(a). To compare the simulated results with the experimental values, the calculated temperature at the center of the circular heater was adjusted to the same temperature values as each measured values by varying the input voltage of the microheater. In Fig. 5(f) (1), the input energy which we used in the experiment was about 20–40 mJ. In Fig. 6(b) (1), the input energy by simulation was 30 mJ. The required energy input was found to be the same order between the experimental value and the simulated value in the
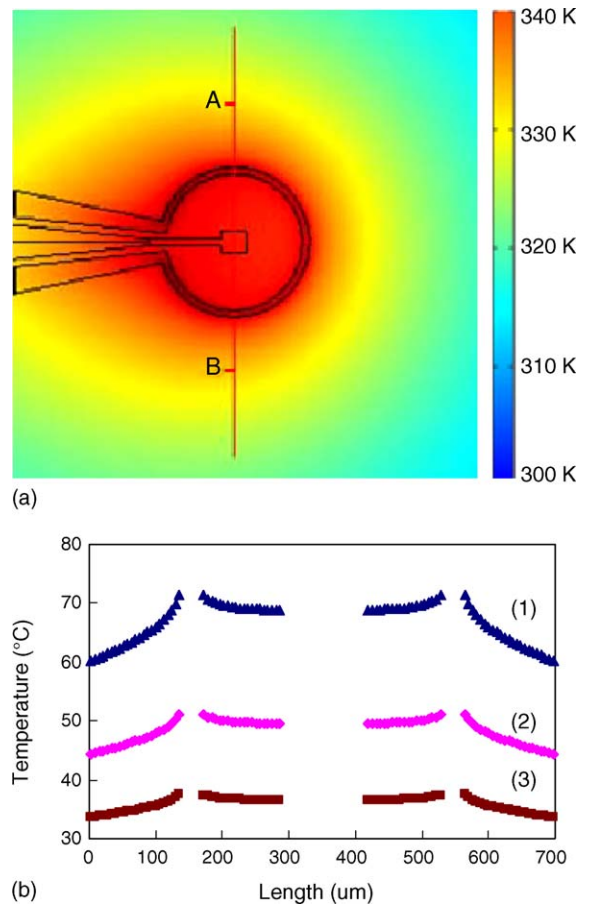

Fig. 6. (a) 2D image of the temperature distribution calculated from the FEM model when the temperature in the center of the device is fixed at 68 °C. (b) Cross-sectional temperature gradients along the red line in (a). The X-axis represents the distance from point A. The areas around 180 μm, from 300 to 400 μm and around 550 μm were subtracted to show the same range as that in Fig. 5. The three plots show the temperature distribution when the center is fixed at 68 °C (1), 51 °C (2) and 37 °C (3), respectively.

same temperature condition. In Fig. 6(b), cross-section plots along the red line of Fig. 6(a) are shown for the three cases. The plots represent the temperature distributions at steady state for each case. A comparison between the temperature distribution and the measured fluorescent intensities, as shown in Fig. 5(f), reveals an excellent agreement between the experiment and simulation.

For further application of the created FEM model, the simplifications made so far might have to be reconsidered. In the current version, we have assumed certain values for the boundary conditions based on literature [12,15]. If we are to make simulations for a deeper study of power consumption and temperature rise time, a thorough investigation should be made to more accurately determine the boundary conditions and the convective heat transfer coefficients [15].

The purpose of the microheater model is two-fold. By comparing the simulation and experimental results the model can serve as an indicator of the accuracy of the proposed measurement technique. In the proposed temperature measurement concept, fluorescent probes are used in combination with a resistive temperature sensor. Based on the temperature at the resistive sensor, the relative intensities from the fluorescent probes are used to determine the temperature distribution over a larger area and with a higher resolution than that possible with only the resistive sensor alone. However, it is important to determine the accuracy of this method and the validity of the observed temperature-dependent fluorescence intensities. Using our theoretical model together with FEMLAB simulations, we obtained results that are in close agreement with the measured values. This let us believe in the usefulness of the proposed technique. Evidently, different experiments such as those involving infrared microscopy or Qdots measurement to determine the temperature distribution, would be useful but more expensive to verify the proposed concept. The second important purpose of the model is that it simplifies the study of parameters such as the material, geometry and applied voltage. Hence, we can predict optimal parameter values and obtain useful information for dealing with important design issues in order to improve factors such as temperature rise time, cooling time and uniform temperature distribution.

6. Application in biomolecular assay

After the temperature distribution was confirmed, the bioassays of a single molecule were conducted inside the circular microheater to show the usefulness of this system and method. Since the accuracy of the microfabricated thermosensor was $1\,^\circ\text{C}$, we could detect the peripheral temperature of the single biomolecule with an accuracy of $3\,^\circ\text{C}$. We demonstrated the rotation assay of a single F1-ATPase, which is a rotary biomolecular motor. A rapid temperature rise times of under 1 s were measured by the integrated thermosensor with an accuracy of $3\,^\circ\text{C}$. The increase in rotation velocity with temperature was observed which indicates that the activity of a single molecule increases with temperature. This temperature detection method allows a precise measurement of activity versus temperature for a single biomolecule in the further study.

7. Conclusion

We have developed a new method to measure the temperature distribution in water with high spatial resolution. This method allows us to detect the temperature of a target under observation with integrated microfabricated thermosensor. Materials for the use of temperature detector was evaluated and carefully selected. Rhodamine B was chosen as a temperature detector due to its reversible calibration curve between temperature and fluorescent intensity. The temperature distribution was successfully calculated from the fluorescent intensity distribution of a rhodamine B solution on the microfabricated thermodevice. Based on the proposed method, direct measurement of local temperatures, which is our area of interest was achieved with an accuracy of $3\,^\circ\text{C}$ and spatial resolution of $5.3\,\mu\text{m}$. FEM modeling was also carried out in order to demonstrate the reliability of this method. A comparison of the measured temperature distribution with the simulated distribution showed an excellent agreement.

A rotation assay of a single F1-ATPase by altering the temperature was conducted simultaneously with precise temperature detection. This was possible for the first time due to the precise temperature distribution measurement around the microfabricated thermodevice. Through continued application of the proposed method in bioassays, new knowledge may potentially be achieved, e.g. the correlation between torque and temperature in a single F1-ATPase. We also performed the temperature distribution measurement in a local area of the glass surface by sandwiching Rhodamine B solution between a glass plate and a PDMS sheet [7]. This experiment precisely measured the temperature of a microchamber which contained certain number of enzymes. This ended up with highly interesting scientific analysis using microfabricated thermodevice. The proposed method is widely applicable for measuring the temperature distribution in local areas, particularly for microchips under the microscope for chemical and biochemical assays.

References

[1] H. Noji, R. Yasuda, M. Yoshida, K. Kinosita Jr., Nature 386 (1997) 299–302.

[2] H. Arata, S. Takeuchi, G. Tresset, Y. Rondelez, K. Tabata, H. Noji, et al., MEMS devices for detecting correspondence between mechanical rotation and ATP consumption in a single biomolecular motor, IEEE MEMS Proc. (2004) 363–366.

[3] H. Arata, S. Takeuchi, H. Noji, H. Fujita, Micro device for local temperature control under microscope, IEEE Trans. SM 124 (8) (2004) (in Japanese).

[4] R. Fortt, A. Iles, A. Mello, Precise control of the Reamer-Tiemann reaction using integrated heating and thermochromic liquid crystals, Proc. μTAS (2003) 267–270.

[5] A. Iles, R. Fortt, A.J. de Mello, Thermal optimization of the Reimer-Tiemann reaction using thermochromic liquid crystals on a microfluidic reactor, Lab Chip 5 (2005) 540–544.

[6] G.W. Walker, V.C. Sundar, C.M. Rudzinski, A.W. Wun, M.G. Bawendi, D.G. Nocera, Quantum-dot optical temperature probes, Appl. Phys. Lett. 83 (17) (2003) 3555–3557.

[7] H. Arata, Y. Rondelez, H. Noji, H. Fujita, Rapid temperature alternation by on-chip micro-heater reveals enzymatic activity of β-galactosidase at high temperatures, Anal. Chem. 77 (2005) 4810–4814.

[8] Y. Rondelez, et al., Microfabricated arrays of femtoliter chambers allow single molecule enzymology, Nat. Biotech. 23 (3) (2005) 361–365.

[9] Y. Rondelez, et al., Highly coupled ATP synthesis by F_1-ATPase single molecules, Nature 433 (7027) (2005) 773–777.

[10] M.N. Slyadnev, Y. Tanaka, M. Tokeshi, T. Kitamori, Photothermal temperature control of a chemical reaction on a microchip using an infrared diode laser, Anal. Chem. 73 (16) (2001) 4037–4044.

[11] Y. Tanaka, M.N. Slyadnev, A. Hibara, M. Tokeshi, T. Kitamori, J. Chromatogr. A 894 (2000) 45–51.

[12] M. Graf, R. Jurischka, D. Barrettino, A. Hierlemann, 3D nonlinear modeling of microhotplates in CMOS technology for use as metal-oxide-based gas sensors, J. Micromech. Microeng. 15 (2005) 190–200.

[13] T. Iwaki, J.A. Covington, F. Uldrea, S.Z. Ali, P.K. Guha, J.W. Gardner, Design and simulation of resistive SOI CMOS micro-heaters for high temperature gas sensors, J. Phys. Conf. Ser. 15 (2005) 27–32.

[14] A. Pike, J.W. Gardner, Thermal modeling and characterization of micropower chemoresistive silicon sensors, Sens. Actuators B 45 (1997) 19–26.

[15] F.P. Incropera, D.P. DeWitt, Introduction to Heat Transfer, third ed., John Wiley & Sons, New York, 1996.

Biographies

Hideyuki Arata was born in Okinawa, Japan, in 1980. He received the BS degree in 2002 and MS degree in 2004 both from Faculty of Engineering and School of Engineering, respectively, at the University of Tokyo. He is currently pursuing a PhD at School of Engineering, the University of Tokyo. He belongs to the laboratory of professor H. Fujita, Institute of Industrial Science, the University of Tokyo, collaborating with professor Hiroyuki Noji. His research topic at Tokyo is "MEMS based microsystems for single biomolecular measurement". He works at Institute Curie, Paris, France, from November 2005 to October 2006 as a visiting scientist in professor Jean-Louis Viovy's group collaborating with Dr. Giovanni Cappello. His current topic at Paris is "single-molecules nanomanipulation, applied to the dynamics of homologous recombination". He received the Incentive Prize at the 1st Invention Contest, the University of Tokyo, 2004. He will assume the post of limited researcher of Japan Society for Promotion of Science from April 2006. He is also acting as a referee of Royal Society of Chemistry, England, especially for the journal *Lab on a Chip*.

Peter Löw received his MSc degree in engineering physics from Lund Institute of Technology (Sweden) in 2004. He is currently assigned as a PhD student to the Laboratory for Analysis and Architecture of Systems (LAAS-CNRS) in Toulouse (France). Through the Japanese–French joint laboratory LIMMS/CNRS-IIS (Laboratory for Integrated Micro Mechatronics Systems), he is a member of the laboratory of professor B.J. Kim at the Institute of Industrial Sciences, the University of Tokyo (Japan), where he conducts research on micro- and nanoscale heating devices for biological applications.

Christian Bergaud was born in Domont, France, in 1968. He received the engineer degree in physics from the National Institute of Applied Sciences, Lyon, France, in 1991 and the PhD degree in electronics from the National Institute of Applied Sciences, Toulouse, France, in 1994. Between 1995 and 1996, he was a postdoctoral fellow with the University of Tokyo, Japan, where he studied the development of microsystems dedicated to metrological applications. From January 1997 to March 2004, he was a National Center of ScientificnResearch (CNRS) researcher with the Laboratory for Analysis and Architecture of Systems (LAAS), Toulouse. In April 2004, he was appointed director of the Laboratory for Integrated Micro Mechatronics Systems, a joint laboratory of the French CNRS and the University of Tokyo. His research involves physical characterization of micro- and nanostructures, and the development of novel approaches to design micro- and nanosystems for biological applications.

Beomjoon Kim received his BE degree from Seoul National University, the Department of Mechanical Design and Production Engineering, Seoul, Korea, in 1993, and received his ME and PhD in precision machinery engineering from the University of Tokyo, Tokyo, Japan, in 1995 and 1998, respectively. He is currently an associate professor of the Institute of Industrial Science, University of Tokyo, Japan, and also co-director of CIRMM/CNRS in Paris. His research interests are microsystems, micromeasurement (SNOM, SPM) and industrial applications of MEMS technology.

Hiroyuki Noji was born in 1969. He received his BS, SM and PhD degree from Tokyo Institute of Technology. He was an associate professor of the Institute of Industrial Science, the University of Tokyo from 2001 to 2005. He is currently a professor at the Institute of Scientific and Industrial Research (ISIR), the Osaka University. His research interest lies in single molecular physiology, biophysics and biochemistry. He received the Grand Prize, Amasam Pharmacia Biotech & Science Prize for Young Scientist in 1998 and Tejima Prize in 1999.

Hiroyuki Fujita received his BS, SM and PhD degree in electrical engineering from the University of Tokyo in 1975, 1977 and 1980, respectively. He was a visiting scientist with the Francis Bitter National Magnet Laboratory, Massachusetts Institute of Technology from 1983 to 1985 for research on superconducting magnets. He is currently a professor of the Institute of Industrial Science, the University of Tokyo. His research interest is micro electro-mechanical systems fabricated by IC-based processes and applications to optics, hard disk drives and biotechnology. He is also interested in autonomous distributed microsystems.